Controlling Diffusive Network Processes Using Incidental Measurements and Actuation

Amirkhosro Vosughi, Mengran Xue, and Sandip Roy

Abstract— **Feedback control of diffusive network dynamics using incidental measurements and actuation is explored. A standard model for diffusion or synchronization in networks is enhanced to represent two incidental control architectures: one in which clocked measurements from a stochastically-moving platform are used to regulate a fixed actuator, and a second where the sensor and actuator are collocated on a moving platform. Simple proportional-integral-derivative control schemes are studied. For both control architectures, low-gain controllers are shown to achieve regulation in a mean-square sense. A simulation example is presented, which demonstrates that the incidental control architectures allow for practical regulation, and in fact can sometimes outperform a fixed control architecture.**

I. INTRODUCTION

The analysis and control of network dynamics have been a primary focus of the controls-engineering community during the last 15-20 years (e.g. [1], [2]). Within this broad effort, there has been a particular interest in the analysis and control of network diffusion and synchronization processes, such as thermal processes in buildings, rumor or disease spread, and distributed clock synchronization, to name just a few [1]–[5]. A major thrust of the work on diffusive networks has been to understand how global coordination emerges from local diffusive interactions, and in turn to design decentralized and distributed control schemes to shape global properties. This research has also been extended toward achieving disturbance rejection, addressing sparse controller design, developing state and mode estimators, and characterizing input-output properties, among many other directions [4], [6]–[9]. A common theme underlying the various studies has been to expose the connection between the network's graph and its dynamics and control.

The deployment and networking of new sensing/actuation technologies are enabling a paradigm shift in the control of complex network dynamics, including diffusive processes [10]–[12]. One aspect of this paradigm shift is the growing availability of ad hoc or *incidental* measurement and actuation platforms, which stochastically probe or actuate the network dynamics while primarily serving other purposes or engaging in unrelated missions [13]–[16]. For instance, personal handheld devices like Smartphones provide a wealth of information on user locations, which can be used for e.g. traffic congestion management or catered control of building

HVAC systems. In a parallel vein, unmanned aerial or underwater vehicles can allow persistent sampling of environmental processes and hazards (e.g., pollution levels), and perhaps can directly combat some hazards. Meanwhile, social-media communications and blogs serve as monitors for the spread of infectious diseases, as well as for human social dynamics. These various platforms are incidental or ad hoc, in the sense that their primary missions are typically unrelated to the sensing and actuation of the diffusive network processes. Despite being stochastic in nature, however, these incidental platforms can greatly inform monitoring and control. Indeed, such platforms have already been widely used for real-time monitoring of network processes like traffic congestion and disease spread. To date, real-time feedback control using these ad hoc platforms has been more limited, perhaps due to the inherent variability of the measurements and actuations permitted by the platforms.

In this article, we explore feedback control of diffusive network processes using ad hoc or incidental measurements and actuations. Specifically, a standard diffusive-network model is augmented to represent two control architectures, one that uses clocked measurements from a stochastically-moving platform along with a fixed actuator, and a second where collocated measurement and actuation from a mobile platform are used (Section II). For both architectures, proportional-integral-derivative (PID) controls are considered, for regulation of the network state. The closed-loop dynamics at sample times are shown to be governed by a discrete-time Markov jump-linear system (Section III.A). This MJLS formulation is used to verify that regulation is achieved asymptotically in a mean-square sense, when low-gain proportional-derivative controllers are applied (Sections III.B and III.C). Finally, a simulation is presented which shows that incidental measurement and actuation-based control schemes are practical, in the sense that they enable faster regulation as compared to fixed schemes.

The research described here builds on two recent studies on incidental measurement paradigms for dynamical networks, one focused on state estimation from Markov and non-Markov measurements from an incidentally-mobile platform [15], the second concerned specifically with feedback control of building thermal processes using incidental measurements [16]. The approach taken here is closely connected to the wide literature on the control of Markov jump-linear systems (MJLS) [17]–[19], including particularly efforts on control of jump-linear network processes [20], [21]. Relative to the literature on MJLS, the main contribution of this work is to show how the special structure of the diffusive

network dynamics can be exploited to construct simple control schemes that achieve regulation.

II. MODELING AND PROBLEM FORMULATION

A standard model for diffusive interactions in a network is enhanced to capture Markov sensing and actuation paradigms. Formally, a network with n nodes, labeled $1, 2, \cdots, n$, is considered. Each node i has associated with it a state $x_i(t)$, which evolves with the continuous time variable t. Each state $x_i(t)$ is governed by the following differential equation

$$\dot{x}_i(t) = \sum_{j=1, j \neq i}^{n} a_{ij}(x_j - x_i) + \gamma_i(t)u(t) \quad (1)$$

where the weights a_{ij} indicate the strengths of the diffusive interactions, the scalar $u(t)$ is a control input, and $\gamma_i(t) \geq 0$ (where $\sum_i \gamma_i(t) = 1$) indicates the (possibly time-varying) actuation level provided to node i due to the control input. The dynamics can be expressed in matrix form as

$$\dot{\mathbf{x}} = A\mathbf{x}(t) + B(t)u(t) \quad (2)$$

where $\mathbf{x} = \begin{bmatrix} x_1 & \cdots & x_{n-1} & x_n \end{bmatrix}^{\mathbf{T}}$, the entry of A at row i and column j is given by $A_{ij} = a_{ij}$ for $i \neq j$, the diagonal entries of A are given by $A_{ii} = -\sum_{j \neq i} a_{ij}$, and $B(t)$ is an $n \times 1$ vector with ith entry equal to $\gamma_i(t)$ for $i = 1, \ldots, n$. We note that the internal dynamics of (2) have been very widely studied, as a model for consensus/synchronization or diffusion in networks.

Two measurement and actuation architectures are considered in this study: 1) an *incidental-measurement architecture*, where measurements from a sensor that is moving stochastically among the nodes are used for feedback control of a fixed actuation capability; and 2) a *mobile sensor-actuator architecture*, where a single stochastically-moving device is responsible for both sensing and actuation at its current location. For both architectures, the movement of a single device among the network's nodes is considered. Noting that measurement and actuation devices are increasingly cyber-enabled, we assume a clocked model for the measurements and/or actuation made by the stochastically- moving device in our framework. Formally, the device's location in the network is modeled as Markov process which evolves at clocked intervals, specifically at the times $t = kT$ for $k = 0, 1, 2, \cdots$. The node occupied by the device at time $t = kT$ is denoted as $s[k]$, where $s[k]$ may take on values among $1, \cdots, n$. The device location $s[k]$ is modeled as a finite-state Markov chain with $(n) \times (n)$ transition matrix $P = \begin{bmatrix} p_{ij} \end{bmatrix}$. This *location Markov chain* is assumed throughout this work to be ergodic.

For both architectures, state measurements are obtained at the device's current location at the clocked intervals, for the purpose of feedback control. Formally, the measurement $y[k]$ is the state of the occupied node sampled at time $t = kT$, i.e. $y[k] = x_{s[k]}(kT)$. For the statistical analysis developed here, it is convenient to express the measurement as a time-varying projection of the state $\mathbf{x}(t)$. Specifically, we have

that $y[k] = \overrightarrow{v}^T[k]\mathbf{x}(kT)$, where $\overrightarrow{v}^T[k]$ is a 0 –1 indicator vector for the occupant's node $s[k]$.

Two actuation paradigms are considered here. For the incidental-measurement architecture, the coefficients $\gamma_i(t)$ and hence input matrix $B(t)$ is fixed. For the mobile measurement and actuation architecture, the control unit is modeled as moving with the sensor to the different network nodes. In that case, the $\gamma_i(t)$ and hence $B(t)$ are time varying. Specifically, noting that the sensor and actuator are collocated, the input matrix $B(t)$ is modeled as $B(t) = B[k]$ for $kT \leq t < (k+1)T$, where $B[k] = \overrightarrow{v}[k]$. We are interested in designing control schemes to regulate the state of diffusive process. Specifically, we seek to design the control so that the node states $x_i(t)$ are regulated to a common desired reference value y_{ref}, i.e. $x_i(t) - y_{ref} \to 0$ for $i = 1, \ldots, n$. From the diffusive form of the model, we notice here that the node states asymptote to a common value even when no control is used, provided that the state matrix A is irreducible; however, the asymptote is governed by the initial states of the network nodes. The aim of the control here is to permit regulation to a desired reference value.

The above described model for incidental measurement/actuation of diffusive network processes is becoming relevant to an array of controller design applications, as new IoT technologies enable pervasive sensing and actuation from user-based platforms like cell phones. Here, we briefly describe two potential applications. First, the model (2) can be used to model thermal processes in buildings, see e.g. our previous work [16] which tracks temperature dynamics is rooms within a building, see also the literature on resistive-capacitive network models for heat flow within buildings [**?**], [**?**]. New IoT-based sensing technologies enable locationing of occupants, whose movement can be modeled as a Markov process, as well as sensing of temperatures throughout the building. Hence, clocked measurements of temperatures in the occupants' current locations are available. A natural control scheme is to regulate the temperature at the occupants' current locations, so as to optimize comfort while saving energy. This problem resolves to a control problem for a diffusive network process with incidental measurements. Air pollution is a second process that can be modeled with linear diffusion model [15]. Unmanned aerial vehicles (drones) can be used to measure the level of air pollution, as they circulate around different areas of city on unrelated missions; thus, incidental measurements are obtained of the diffusion process. Some drones may also have technologies that enable local actuation of the pollution process, e.g. via dispersion of cleaning agents. Similar incidental-measurement-based and mobile-sensor-actuator-based controls can be envisioned for other diffusive processes like oil spills and spreads of infectious diseases.

In this work, a proportional-integral-derivative control scheme is considered, since simple and generic schemes are practical for many mobile-control applications. We consider implementation of the control via a zero-order-hold, for which the control input is updated after each data transmission and held constant in between. The following PID control

scheme of this form is proposed:

$u(t) = u[k]$ for $kT \leq t < (k+1)T$, where:

$u[k] = K_p(y_{ref} - y[k]) + K_d(y[k] - y[k-1])/T + K_i \sum_0^k (y_{ref} - y[k]) \times T$

and where K_p, K_d and K_i are proportional, derivative, and integral gains.

The main focus of this work is to develop a statistical analysis of the closed-loop dynamics of the diffusion process for two incidental control architectures, and to use the analysis to show that the control achieves regulation. Via simulations, the incidental sensing and actuation schemes are compared with fixed schemes, with regard to the speed at which regulation is achieved.

III. CONTROLLER ANALYSIS AND DESIGN

The main purpose of this section is to develop a two-moment statistical analysis of the closed-loop dynamics for both incidental measurement/actuation paradigms, and in turn to demonstrate that low-gain controls can be designed to achieve the regulation goal. The notation and approach of this part is highly related to our previous attempt in [16]. However, here we concern about general diffusion process rather than heat flow problem that was discussed in [16]. That means our $\bar{A}$ matrix is laplacian in this work rather than grounded laplacian with was in [16]. Also low gain stability results are expanded for PID controller through theorem 5 and 6 in this work.

The analysis and design are approached as follows. First, the closed-loop state dynamics sampled at the data-transmission times are reformulated as a discrete-time Markov jump-linear system or MJLS (III.A). Standard results for MJLS are then used to develop a two-moment analysis of the state dynamics (Section III.B). An eigenanalysis of the moment dynamics is undertaken to demonstrate stochastic (two-moment) stability, and in turn to verify that regulation is achieved (Section III.C): this is the main technical contribution of the paper. We note that a preliminary statistical analysis of an incidental-measurement-based feedback control for building thermal processes was developed without proof in the brief paper [16]. The preliminary analysis in Sections III.A and III.B partially follows this development, however the main stability analysis is new and also the methodology is generalized to encompass the mobile sensor-actuator architecture.

A. Reformulation as an MJLS

For both control architectures, the closed-loop dynamics sampled at the data-transmission times are shown to be governed by an autonomous discrete-time state equation whose state matrix switches according to the Markov chain, i.e. the dynamics are reformulated as an autonomous MJLS. This reformulation requires defining an extended state vector $\overrightarrow{\xi}$, as: $\overrightarrow{\xi}[k] = \begin{bmatrix} \overrightarrow{\theta}[k] \\ \overrightarrow{\theta}[k-1] \\ Acc[k] \end{bmatrix}$ where $\overrightarrow{\theta}[k] = \overrightarrow{x}[k] - y_{ref}\overrightarrow{1}$ is a shift of the state vector relative to the desired (goal) state, $\overrightarrow{1}$ is a vector with all unity entries, $Acc[k] = \sum_{m=1}^k z[k]$ is

an accumulator for the integral controller, and $z[k] = \overrightarrow{v}^T \overrightarrow{\theta}$ indicates the diffusive proces state at the device location in the shifted coordinates.

The extended state vector $\overrightarrow{\xi}[k]$ is governed by a discrete-time MJLS model, which can be obtained by solving the continuous-time diffusive dynamics over intervals of duration T for each possible underlying observer-location state:

$$\overrightarrow{\xi}[k+1] = G_c^{PID}(i)\overrightarrow{\xi}[k] \qquad (3)$$

where the $(2n+1) \times (2n+1)$ matrix $G_c^{PID}(i)$ is function of the location Markov chain state i. The matrix $G_c^{PID}(i)$, $i = 1, \ldots, n$, can be calculated as follows:

$$G_c^{PID}(i) = G_A^{PID}(i) + G_p^{PID}(i) + G_d^{PID}(i) + G_i^{PID}(i) \quad (4)$$

where

$$G_A^{PID}(i) = \begin{bmatrix} \bar{A} & 0_{n\times n} & 0_{n\times 1} \\ I_{n\times n} & 0_{n\times n} & 0_{n\times 1} \\ v^T(i) & 0_{1\times n} & 1 \end{bmatrix}$$

$$G_p^{PID}(i) = -K_p\Phi_{\bar{\beta}} \begin{bmatrix} S_2(i) & 0_{n\times n} & 0_{n\times 1} \\ 0_{n\times n} & 0_{n\times n} & 0_{n\times 1} \\ 0_{1\times n} & 0_{1\times n} & 0 \end{bmatrix}$$

$$G_d^{PID}(i) = \frac{-K_d}{T}\Phi_{\bar{\beta}} \begin{bmatrix} S_2(i) & -S_2(i) & 0_{n\times 1} \\ 0_{n\times n} & 0_{n\times n} & 0_{n\times 1} \\ 0_{1\times n} & 0_{1\times n} & 0 \end{bmatrix}$$

and

$$G_i^{PID}(i) = -K_i T\Phi_{\bar{\beta}} \begin{bmatrix} S_2(i) & 0_{n\times n} & 1_{n\times 1} \\ 0_{n\times n} & 0_{n\times n} & 0_{n\times 1} \\ 0_{1\times n} & 0_{1\times n} & 0 \end{bmatrix}.$$

Here, $\bar{A} = e^{AT}$, S_2 is an $n \times n$ matrix whose ith column is a unity vector while all other entries are 0, and $\Phi_{\bar{\beta}}$ is $(2n+1) \times (2n+1)$ diagonal matrix. For the incidental-measurement control architecture, for each i, the jth diagonal entry of $\Phi_{\bar{\beta}}$ is equal to jth entry of the vector $\Phi_\beta = \Phi B$ for $j = 1, \ldots, n$, where $\Phi = \int_0^T e^{A(\tau)}d\tau$. For the mobile measurement and actuation architecture, the jth diagonal entry of $\Phi_{\bar{\beta}}$ is equal to the jth entry of the vector $\Phi_\beta = \Phi e_i$ for $j = 1, \ldots, n$ where $\Phi = \int_0^T e^{A(\tau)}d\tau$, and e_i is a 0–1 indicator vector whose ith entry is unity.

The matrix $G_A^{PID}(i)$ in the above expression describes the nominal (uncontrolled) diffusive dynamics and the evolution of the accumulator state $Acc[k]$, while $G_p^{PID}(i)$, $G_d^{PID}(i)$ and $G_i^{PID}(i)$ describe the effects of the proportional, derivative, and integral control terms, respectively.

A simpler approximation of the MJLS formulation can be obtained, provided that the time-constants of the diffusion process are large compared to the sampling (data-transmission) interval T, which is the case for many diffusive processes. The approximation is appealing for computational purposes, and also because the graph structure of the diffusion process is then explicitly encoded in the matrices $G_c^{PID}(i)$. We primarily focus on the exact model here, but include the approximation for these reasons. Specifically, provided that T is sufficiently small, the matrix exponential e^{AT} can be approximated as $e^{AT} = I + TA$. In this case, the summed matrices in Equation 4 can be approximated as:

$$G_A^{PID}(i) = \begin{bmatrix} I + TA & 0_{n\times n} & 0_{n\times 1} \\ I_{n\times n} & 0_{n\times n} & 0_{n\times 1} \\ v^T(i) & 0_{1\times n} & 1 \end{bmatrix}$$

$$G_p^{PID}(i) = -K_p S_1 \begin{bmatrix} S_2(i) & 0_{n\times n} & 0_{n\times 1} \\ 0_{n\times n} & 0_{n\times n} & 0_{n\times 1} \\ 0_{1\times n} & 0_{1\times n} & 0 \end{bmatrix}$$

$$G_d^{PID}(i) = \frac{-K_d}{T} S_1 \begin{bmatrix} S_2(i) & -S_2(i) & 0_{n\times 1} \\ 0_{n\times n} & 0_{n\times n} & 0_{n\times 1} \\ 0_{1\times n} & 0_{1\times n} & 0 \end{bmatrix}$$

$$G_i^{PID}(i) = -K_i T S_1 \begin{bmatrix} S_2(i) & 0_{n\times n} & 1_{n\times 1} \\ 0_{n\times n} & 0_{n\times n} & 0_{n\times 1} \\ 0_{1\times n} & 0_{1\times n} & 0 \end{bmatrix}.$$

For the incidental-measurements architecture, S_1 is a $(2n+1) \times (2n+1)$ diagonal matrix whose jth diagonal entry is equal to γ_j for $j = 1, \ldots, n$ (and whose remaining diagonal entries are zero). For the mobile measurement and actuation architecture, S_1 is a $(2n+1) \times (2n+1)$ diagonal matrix whose ith diagonal entry is unity (and all other diagonal entries are zero).

B. Two-Moment Analysis

Standard analyses of state moments for MJLS can be applied to find statistics of the closed-loop dynamics of the diffusive network model, for either control architecture [17]–[19]. Specifically, a two-moment analysis requires consideration of the Kronecker product vectors $\psi_1[k] = \overrightarrow{v}^T[k] \otimes \xi[k]$ and $\psi_2[k] = \overrightarrow{v}^T[k] \otimes \xi[k]^{\otimes 2}$, which contain products of the extended state vector entries with an indicator of the underlying Markov chain's status. Here, the notation $(Q)^{\otimes 2}$ refers to the self-Kronecker product of the matrix or vector Q. The vectors $\psi_1[k]$ and $\psi_2[k]$ have $n(2n+1)$ and $n(2n+1)^2$ entries, respectively. From the standard MJLS analysis [17]–[19], the *first-moment vector* $E(\psi_1[k])$ and the *second-moment vector* $E(\psi_2[k])$ are governed by the following linear time-invariant dynamics: $E(\psi_1[k+1]) = H_1^{PID} E(\psi_1[k])$,

where $H_1^{PID} = \begin{bmatrix} p_{11} G_c^{PID}(1) & \cdots & p_{1n} G_c^{PID}(n) \\ \vdots & \ddots & \vdots \\ p_{n1} G_c^{PID}(1) & \cdots & p_{nn} G_c^{PID}(n) \end{bmatrix}$.

Likewise, $E(\psi_2[k+1]) = H_2^{PID} E(\psi_2[k])$, where $H_2^{PID} =$
$\begin{bmatrix} p_{11} G_c^{PID}(1)^{\otimes 2} & \cdots & p_{1n} G_c^{PID}(n)^{\otimes 2} \\ \vdots & \ddots & \vdots \\ p_{n1} G_c^{PID}(1)^{\otimes 2} & \cdots & p_{nn} G_c^{PID}(n)^{\otimes 2} \end{bmatrix}$.

We notice that the first and second moment vectors contain conditional moments of the extended state vector, given the measurement location. For example, the first moment vector can be written as $E(\psi_1[k]) = \begin{bmatrix} E(\xi[k]|s[k]=1)P(s[k]=1) \\ \vdots \\ E(\xi[k]|s[k]=n)P(s[k]=n) \end{bmatrix}$, where $E(\xi[k]|s[k]=j)$ is the conditional expectation of the extended state given the measurement/actuation device's location, and $P(s[k]=j)$ is the location probability at time step k.

C. Stability Analysis

It is shown that the first and second moment dynamics of the MJLS are asymptotically stable when low-gain pro-

portional (P), proportional-derivative (PD), or proportional-integral-derivative (PID) feedback control are used, for both control architectures. Hence, the expected squared deviation of each node's state from the desired reference, i.e. $E((x_i(t) - y_{ref})^2)$ for $i = 1, \cdots, n$, approaches zero asymptotically. The stability analysis serves as a verification that the two incidental control architectures indeed can be used to regulate diffusive processes, in such a way that the state at all network locations tracks a specified constant reference signal.

The stability analysis is based on an eigenanalysis of the recursion matrices H_1^{PID} and H_2^{PID}, which draws on the structure of the diffusive network dynamics. The state matrices for the first- and second- moment dynamics for the uncontrolled diffusive network model each have a single eigenvalue at 1 (provided that the network graph is strongly connected), with the remaining eigenvalues located strictly within the unit circle. Our focus is on understanding whether the moment dynamics of the MJLS are strictly (asymptotically) stable, with eigenvalues strictly within the unit circle, when the two incidental measurement/actuation-based control schemes are deployed. In the following theorems, asymptotic stability of the moment dynamics are verified, and in turn the regulation goal is shown to be achieved exactly in a mean-square sense, for low-gain proportional (P), proportional-derivative (PD), and proportional-integral-derivative (PID) controls. The results are developed in detail for the incidental-measurement control architecture, and analogous results are then summarized for the mobile sensor-and-actuator architectures. Although the result for the PID controller encompasses the results for the P and PD controller, we present the three results sequentially to simplify the presentation of their proofs, which build on each other. The separate treatment of the different control architectures also yields explicit formulas for eigenanalysis of the moment recursions for these special controls. The proofs of the theorems draw on results for non-negative matrices [22], [23]. The first result addresses proportional control when the incidental-measurement architecture is used.

Theorem 1: Consider the closed-loop diffusion process in the case that the nodes are connected, and the location Markov chain is ergodic. Consider the incidental measurement control architecture, and assume that a proportional control is used (i.e. $K_d = K_i = 0$). For all sufficiently small negative feedback ($0 \leq K_p \leq \bar{K}_p$, for some $\bar{K}_p > 0$), the first- and second- moment dynamics for the MJLS formulation are asymptotically stable in the sense of Lyapunov. Further, regulation is achieved, i.e. $\mathbf{x}(t) - y_{ref}\mathbf{1}$ approaches the origin in a mean-square sense.

Proof:

When a proportional controller is used, the MJLS formulation only requires tracking the shifted state vector $\overrightarrow{\theta}[k]$ at the data-transmission times. The shifted state vector is

governed by the autonomous discrete-time MJLS:

$$\overrightarrow{\theta}[k+1] = G_c^P(i)\,\overrightarrow{\theta}[k], \qquad (5)$$

where the $n \times n$ matrix $G_c^P(i)$ is given by:

$$G_c^P(i) = G_A^P(i) + G_p^P(i) \qquad (6)$$

where $G_A^P(i) = \bar{A}$ and $G_p^P(i) = -K_p \Phi S_2(i)$, and where the parameters in the equations are as defined before.

For the proportional controller, the two-moment analysis of the discrete-time closed-loop model can be developed using the Kronecker product vectors $\chi_1[k] = \overrightarrow{v}^T[k] \otimes \theta[k]$ and $\chi_2[k] = \overrightarrow{v}^T[k] \otimes \theta[k]^{\otimes 2}$. Per the standard analysis of MJLS, the *first-moment vector* $E(\chi_1[k])$ and the *second-moment vector* $E(\chi_2[k])$ are governed by the following linear dynamics: $E(\chi_1[k+1]) = H_1^P E(\chi_1[k])$,

where $H_1^P = \begin{bmatrix} p_{11}G_c^P(1) & \cdots & p_{1n}G_c^P(n) \\ \vdots & \ddots & \vdots \\ p_{n1}G_c^P(1) & \cdots & p_{nn}G_c^P(n) \end{bmatrix}$; and

$E(\chi_2[k+1]) = H_2^P E(\chi_2[k])$, where $H_2^P = \begin{bmatrix} p_{11}G_c^P(1)^{\otimes 2} & \cdots & p_{1n}G_c^P(n)^{\otimes 2} \\ \vdots & \ddots & \vdots \\ p_{n1}G_c^P(1)^{\otimes 2} & \cdots & p_{nn}G_c^P(n)^{\otimes 2} \end{bmatrix}$. The matrix H_1^P has dimension equal to $n^2 \times n^2$, while the matrix H_2^P has dimension equal to $n^3 \times n^3$.

To prove that the linear dynamics governing the first- and second- moments are stable in the sense of Lyapunov, we will show that H_1^P and H_2^P have eigenvalues strictly inside the unit circle, for sufficiently small k_p. This is proved according to the following four steps.

Step 1: Several properties of the matrices $G_c^P(i)$ are determined. First note that $G_c^P(i) = \bar{A} - K_p \Phi S_2(i)$, where $\bar{A} = e^{TA}$. The matrix A is a Metzler-matrix with zero row sum. Since sum of each row A is equal to zero. It is immediate that A has a non-repeated eigenvalue at 0 with right eigenvector $\overrightarrow{1}$, with remaining eigenvalues strictly in the ORHP. Using the Jordan decomposition of A to find the matrix exponential, it thus follows that $\bar{A} = e^{TA}$ has a non-repeated eigenvalue at 1 with right eigenvalue $\overrightarrow{1}$, and hence the row sums of e^{TA} are 1. Since A is a non-singular irreducible Metzler matrix, it follows immediately that $\bar{A} = e^{AT}$ is strictly positive [22], [23]. Also, notice that $-K_p \Phi S_2(i)$ has strictly negative entries in row $1, \dots, n$ of the ith column, and is zero otherwise. Further, for any sufficiently small positive K_p (less than some $\bar{K}_p$), the entries in the ith column of $-K_p \Phi S_2(i)$ are strictly less than the entries in the ith column of $\bar{A}$ in magnitude. Thus, it follows immediately that where $G_c^P(i)$ is nonnegative with row sums less than or equal to 1, and one row sum strictly less than one.

Step 2: From this point on (Steps 2-3), we investigate the properties of H_1^P and H_2^P based on the obtained properties of $G_c^P(i)$. For the case that $K_p = 0$, this implies $G_c^P(i) = \bar{A}$. In that case, the sum of each row of H_1^P is equal to one and all entries are positive. Therefore, H_1^P has one eigenvalue equal to one and the remaining eigenvalues are inside the unit circle. Now consider the graph representation of H_1^P. From

the expression for H_1^p, the vertices in this graph form a single recurrent class, since P is ergodic and A is fully connected. Now consider the matrix H_1^p and its corresponding graph when a negative feedback is used. For sufficiently small negative gains K_p ($0 < K_p < \bar{K}_p$ for some $\bar{K}_p$), the matrix H_1^p continues to be nonnegative and the graphs continues to contain a single recurrent class. Further, some entries in H_1^P decreased compared to the uncontrolled case, and hence at least one row in H_1^P has row sum less than 1. Thus, the dominant eigenvalue of H_1^P is strictly less than 1 and magnitude, and all eigenvalues of H_1^P are verified to be located strictly inside the unit circle.

Step 3: An entirely analogous argument can be used to prove that H_2^P has a single eigenvalue at 1, with other eigenvalues strictly within the unit circle for uncontrolled case. The proof for H_2^P requires verifying that $G_c^P(i)^{\otimes 2}$ has nonnegative entries and row sums are less or equal than 1. These properties follow immediately from an expansion of the Kronecker product, whereupon the analogous logic as Steps 1-2 can be used to characterize the spectrum.

The eigenstructures of H_1^P and H_2^P show that the linear recursions for the first- and second- moment vectors are asymptotically stable in the sense of Lyapunov, and hence $\chi_1[k]$ and $\chi_2[k]$ for $k = 0, 1, 2 \dots$ are upper bounded and asymptotically decaying to the origin. Since the first- and second- moments of $x[k] - y_{ref}\mathbf{1}$ are purely linear functions of $\chi_1[k]$ and $\chi_2[k]$, the moments are also verified to be bounded and decaying to the origin. It remains to show that the expected squared deviation $E((\mathbf{x}(t) - y_{ref}\mathbf{1})^T(\mathbf{x}(t) - y_{ref}\mathbf{1}))$ is bounded for all $t \geq 0$, and further asymptotes to the origin. To see why this is true, notice that $\mathbf{x}(t) - y_{ref}\mathbf{1}$ is a purely linear function of $\mathbf{x}[k^*] - y_{ref}\mathbf{1}$, where k^* is greatest integer less than $\frac{t}{T}$. Since $\mathbf{x}(t) - y_{ref}\mathbf{1}$ is computed from $x[k^*]$ by solving the closed-loop system over the interval $[k^*T, t]$, where $t < (k^* + 1)T$, it follows that the linear mapping between $x[k^*] - y_{ref}\mathbf{1}$ and $\mathbf{x}(t) - y_{ref}\mathbf{1}$ is uniformly bounded. Thus, it follows that the expected squared deviation $E((\mathbf{x}(t) - y_{ref}\mathbf{1})^T(\mathbf{x}(t) - y_{ref}\mathbf{1}))$ is bounded for all $t \geq 0$, and further asymptotes to the origin.

∎

An analogous result can be obtained for the mobile sensor and actuator model, when proportional control is used:

Theorem 2: Consider the closed-loop diffusion process in the case that the nodes are connected, and the location Markov chain is ergodic. Consider the mobile sensor and actuator architecture, and assume that a proportional control is used (i.e. $K_d = K_i = 0$). For all sufficiently small negative feedback ($0 \leq K_p \leq \bar{K}_p$, for some $\bar{K}_p > 0$), the first- and second- moment dynamics for the MJLS formulation are asymptotically stable in the sense of Lyapunov. Further, regulation is achieved, i.e. $\mathbf{x}(t) - y_{ref}\mathbf{1}$ approaches the origin in a mean-square sense.

The proof for the result is identical to that for the incidental-measurement architecture, with only the change that different entries in $G_c^P(i)$ are decreased when a negative feedback is applied. Since the proof is so similar, it is

omitted.

We remark that for a small positive gain k_p, the moment vector dynamics are necessarily unstable. This is because the sum of some rows of H_1^P and H_2^P exceed 1 while all other rows sum to 1, and therefore H_1^P and H_2^P must have eigenvalues outside the unit circle.

Theorems 1 and 2 establish that all low-gain zero-order-hold proportional control schemes achieve asymptotic stability of the first two moments, and hence that the expected squared deviation between the state the reference signal approaches zero in a mean-square sense. The theorem is important as a verification that incidental measurement/actuation-based platforms can be used to regulate diffusive processes, and serves as a starting point for tuning the gains to achieve desired performance specifications or optimizing performance tradeoffs.

Stability can also be verified for all low-gain proportional-derivative control schemes, as formalized in the following theorems:

Theorem 3: Consider the closed-loop diffusion dynamics in the case that the nodes are connected, and the location Markov chain is ergodic. Consider the incidental measurement control architecture, and assume that a proportional-derivative control is used (i.e. $K_i = 0$). For all sufficiently small negative feedback policies ($0 \leq K_p \leq \bar{K}_p$ and $0 \leq K_d \leq \bar{K}_d$, for some $\bar{K}_p > 0$ and $\bar{K}_d > 0$), the first and second moment vectors are governed by linear systems that are asymptotically stable in the sense of Lyapunov. Further, regulation is achieved, i.e. $\mathbf{x}(t) - y_{ref}\mathbf{1}$ approaches the origin in a mean-square sense.

Proof:

The proof for the proportional-derivative controller builds on the proof for the proportional control, hence only the required additional steps are presented.

For the PD controller, reformulation of the sampled dynamics as an autonomous MJLS requires tracking the extended state vector $\overrightarrow{\eta}[k] = \begin{bmatrix} \overrightarrow{\theta}[k] \\ \overrightarrow{\theta}[k-1] \end{bmatrix}$. The two-moment analysis of the discrete-time closed-loop model can then be developed using the Kronecker product vectors $\varrho_1[k] = \overrightarrow{\upsilon}^T[k] \otimes \eta[k]$ and $\varrho_2[k] = \overrightarrow{\upsilon}^T[k] \otimes \eta[k]^{\otimes 2}$. The expectations of these vectors are governed by linear dynamics: $E(\varrho_1[k+1]) = H_1^{PD} E(\varrho_1[k])$ and $E(\varrho_2[k+1]) = H_2^{PD} E(\varrho_2[k])$, Aymptotic stability of the first and second moment dynamics, in the sense of Lyapunov, again can be assured by showing H_1^{PD} and H_2^{PD} has eigenvalues strictly within the unit circle for $0 < K_p < \bar{K}_p$ and $0 < K_d < \bar{K}_d$.

Let us now consider the graph for the nonnegative matrix H_1^{PD}. From the expression for H_1^{PD} (omitted to save space), this graph is seen to contain a recurrent class of vertices, comprising vertices $1 + 2n(z-1), \dots, n + 2n(z-1)$ for $z = 1, \cdots, n$. The sum of each row of H_1^{PD} corresponding to the recurrent vertices is equal to one for $K_p = K_d = 0$. Also, H_1^{PD} can be permuted to an upper triangular form, such that the submatrix associated with the recurrent class is in the upper left of the matrix. Thus, for the uncontrolled

network, H_1^{PD} has a single eigenvalue equal to one, while the remaining eigenvalues are strictly within the unit circle. For $0 < K_p < \bar{K}_p$ and $0 < K_d < \bar{K}_d$, it is easy to check that entries in the top-left submatrix corresponding to the recurrent class are decreased; further, the entries decreased are strictly positive. It thus follows that, for sufficiently small $\bar{K}_p$ and $\bar{K}_d$, the matrix H_1^{PD} is a nonnegative matrix with a single recurrent class. Further, all rows of of H_1^{PD} corresponding to recurrent vertices have row sum less than or equal to 1, and at least one row has row sum less than 1. It thus follows that, in the closed loop, the dominant eigenvalue of H_1^{PD} is strictly less than 1 in magnitude. A similar argument can be used to show that the dominant eigenvalue of H_2^{PD} is strictly less than 1 in magnitude.

The remainder of the proof follows that for the proportional controller. ∎

An analogous result can be obtained for the mobile measurement-actuation control architecture. The result is presented next (without proof, since it is very similar to that for the incidental measurement architecture):

Theorem 4: Consider the closed-loop diffusion dynamics in the case that the nodes are connected, and the location Markov chain is ergodic. Consider the mobile sensor-actuator control architecture, and assume that a proportional-derivative control is used (i.e. $K_i = 0$). For all sufficiently small negative feedback policies ($0 \leq K_p \leq \bar{K}_p$ and $0 \leq K_d \leq \bar{K}_d$, for some $\bar{K}_p > 0$ and $\bar{K}_d > 0$), the first and second moment vectors are governed by linear systems that are asymptotically stable in the sense of Lyapunov. Further, regulation is achieved, i.e. $\mathbf{x}(t) - y_{ref}\mathbf{1}$ approaches the origin in a mean-square sense.

Theorems 3 and 4 verify that low-gain PD controllers achieve regulation in a mean-square sense. The results show that arbitrary choices of the proportional and derivative feedback gains can be chosen, provided that they are sufficiently small. This freedom to choose the proportional and derivative gains at will means that stabilizing designs can be obtained even if the diffusion process is incompletely modeled. The stability analyses do not directly provide a comparison of the P and PD schemes, but intuitively one might expect that the derivative term would generally allow for faster regulation without overshoot.

The behavior of low-gain PID controllers is more sophisticated, and the integral control gain has to be chosen appropriately (specifically, sufficiently small compared to the proportional and derivative gains) to ensure that regulation is achieved; The following theorem verifies that appropriately-designed low-gain PID controllers also achieve asymptotic stability of the moments, and hence enable regulation.

Theorem 5: Consider the closed-loop diffusion dynamics in the case that the nodes are connected, and the location Markov chain is ergodic. Consider the incidental measurement control architecture, and assume that a proportional-derivative-integrator control is used. Consider applying a small negative proportional and derivative feedback ($0 \leq K_p \leq \bar{K}_p$ and $0 \leq K_d \leq \bar{K}_d$, for some $\bar{K}_p > 0$ and

$\bar{K}_d > 0$). Further assume that a negative integral feedback is applied, which is small compared to the proportional and integral feedback terms ($0 \leq K_i \leq f\min(K_p, K_d)$, for $0 \leq f \leq \bar{f}$ for some $\bar{f}$). the first and second moment vectors are governed by linear systems that are asymptotically stable in the sense of Lyapunov. Further, regulation is achieved, i.e. $\mathbf{x}(t) - y_{ref}\mathbf{1}$ approaches the origin in a mean-square sense.

Proof: The proof is based on results in previous theorems together with an eigenvalue sensitivity or singular perturbation analysis. To develop the proof, we notice that the closed-loop MJLS state matrix when the PID controller is used can be expressed in terms of that for the PD controller, as follows: $G_c^{PID}(i) = \begin{bmatrix} \bar{G}_c^{PD}(i) & \bar{\epsilon}(i) \\ \overrightarrow{V}(i) & 1 \end{bmatrix}$ where $\bar{G}_c^{PD}(i) = G_c^{PD}(i) - \epsilon\bar{O}$, $\epsilon = K_i T$, and $\bar{O}$ is $2n \times 2n$ matrix with all entries equal to one except the first n entries of row i which are equal to corresponding entries of $B'(i)$. Also, $\bar{\epsilon}(i)$ is column vector with $2n$ entries which all equal zero except the ith entry, which is equal to $-\epsilon$. Also, $\overrightarrow{V}(i)$ is row vector with $2n$ entries, whose ith entry is equal to 1 and remaining entries are zero. In Theorem 3, it was shown that all eigenvalues of G_c^{PD} are in unit circle for small K_p and K_d. If we choose K_i sufficiently small compared to K_p and K_d, then all entries of $\bar{G}_c^{PD}$ will remain positive, and further all eigenvalues of $\bar{G}_c^{PD}$ will remain in unit circle as well.

If we substitute the above form of the matrix $G_c^{PID}(i)$ into H_1^{PID}, we have:

$$H_1^{PID} = \begin{bmatrix} p_{11}\begin{bmatrix} \bar{G}_c^{PD}(1) & \bar{\epsilon}(1) \\ \overrightarrow{V}(1) & 1 \end{bmatrix} & \cdots & p_{1b}\begin{bmatrix} \bar{G}_c^{PD}(n) & \bar{\epsilon}(n) \\ \overrightarrow{V}(n) & 1 \end{bmatrix} \\ \vdots & \ddots & \vdots \\ p_{b1}\begin{bmatrix} \bar{G}_c^{PD}(1) & \bar{\epsilon}(1) \\ \overrightarrow{V}(1) & 1 \end{bmatrix} & \cdots & p_{bb}\begin{bmatrix} \bar{G}_c^{PD}(n) & \bar{\epsilon}(n) \\ \overrightarrow{V}(n) & 1 \end{bmatrix} \end{bmatrix} \tag{7}$$

By permuting H_1^P appropriately, we can simplify the eigenanalysis of the matrix. In order to do that, we define $\tilde{H}_1^{PID}$ as a permutation of H_1^{PID}, where the rows and columns $(2n+1)z_1$, $z_1 = 1, \ldots, n$, are placed at the bottom and right of the matrix respectively. Therefore, $\tilde{H}_1^{PID}$ can be written as follows:

$$\tilde{H}_1^{PID} = \begin{bmatrix} F_1 & \tilde{\epsilon} \\ \tilde{V} & P \end{bmatrix} \tag{8}$$

where $F_1 = \begin{bmatrix} p_{11}\bar{G}_c^{PD}(1) & \cdots & p_{1n}\bar{G}_c^{PD}(n) \\ \vdots & \ddots & \vdots \\ p_{n1}\bar{G}_c^{PD}(1) & \cdots & p_{nn}\bar{G}_c^{PD}(n) \end{bmatrix}$ and $\tilde{\epsilon} = \begin{bmatrix} p_{11}\bar{\epsilon}(1) & \cdots & p_{1n}\bar{\epsilon}(n) \\ \vdots & \ddots & \vdots \\ p_{n1}\bar{\epsilon}(1) & \cdots & p_{nn}\bar{\epsilon}(n) \end{bmatrix}$ and $\tilde{V} = \begin{bmatrix} p_{11}\overrightarrow{V}(1) & \cdots & p_{1n}\overrightarrow{V}(n) \\ \vdots & \ddots & \vdots \\ p_{n1}\overrightarrow{V}(1) & \cdots & p_{nn}\overrightarrow{V}(n) \end{bmatrix}$.

If ϵ is equal to zero (i.e. no integral term is used), then $\tilde{H}_1^{PID}$ has lower triangular structure and its eigenvalues are equal to the union of the eigenvalues of F_1 and P. It is easy to show all eigenvalues of F_1 are inside the unit circle because it is positive matrix with all row sums less than

1. Also P has one eigenvalue equal to one, and remaining eigenvalues equal to zero. On the other hand, If K_i and hence ϵ is sufficiently small, from the eigenvalue perturbation theory, we expect the eigenvalues of $\tilde{H}_1^{PID}$ to be close to the eigenvalues prior to perturbation, and hence all eigenvalues except the eigenvalue at 1 necessarily remain within the unit circle. It remains to prove that the eigenvalue of $\tilde{H}_1^{PID}$ at 1 for $\epsilon = 0$, moves into the unit circle for sufficiently small positive ϵ. This can be shown using an eigenvalue sensitivity analysis. Using the fact that the matrix $\tilde{H}_1^{PID}$ is nonnegative for $\epsilon = 0$, both left and right eigenvectors associated with the unity eigenvalue are seen to be nonnegative. Indeed, it can be seen from the reducibility structure of $\tilde{H}_1^{PID}$ that the final m entries of the right eigenvector are strictly positive, while all entries of the left eigenvector are strictly positive. Also, $\tilde{\epsilon}$ is non-positive for non-zero ϵ. Therefore we can argue from the eigenvalue sensitivity formulate that eigenvalues strictly decrease for sufficiently small K_i. Exactly same argument can be applied to H_2^{PID}. The remainder of the proof is similar to that for Theorem 1 and 3, and hence is omitted.

∎

Again, a similar result can be obtained for the mobile sensor-actuator control architecture. The result is presented next (without proof, since it is very similar to that for the incidental measurement architecture):

Theorem 6: Consider the closed-loop diffusion dynamics in the case that the nodes are connected, and the location Markov chain is ergodic. Consider the mobile sensor-actuator control architecture, and assume that a proportional-derivative-derivative control is used. Consider applying a small negative proportional and derivative feedback ($0 \leq K_p \leq \bar{K}_p$ and $0 \leq K_d \leq \bar{K}_d$, for some $\bar{K}_p > 0$ and $\bar{K}_d > 0$). Further assume that a negative integral feedback is applied, which is small compared to the proportional and integral feedback terms ($0 \leq K_i \leq f\min(K_p, K_d)$, for $0 \leq f \leq \bar{f}$ for some $\bar{f}$). Then the first and second moment vectors are governed by linear systems that are asymptotically stable in the sense of Lyapunov. Further, regulation is achieved, i.e. $\mathbf{x}(t) - y_{ref}\mathbf{1}$ approaches the origin in a mean-square sense.

The stability analyses developed in this section verify that PID controllers can be applied to incidental measurement and actuation based architectures for controller diffusive processes. These analyses provide a foundation for designing PID controllers to regulate diffusive processes: a natural next step is to study tuning of the controller gains to achieve desirable performance. Another interesting direction of further work is to relate the performance to the graph topology of the diffusion process, and the Markov model for the sensing/actuation platform. Also, it is important to stress that the moment stability analyses exploit the diffusive structure of the network dynamics; the verification that low-gain controllers with incidental measurements/ actuation stabilize such diffusive processes is the main result of this study.

IV. EXAMPLE

The control of a linear diffusive network using incidental measurements and/or actuation is illustrated in a small example. Specifically, the two control architectures studied in the paper are compared with a fixed scheme.

A network with 7 nodes, which are connected as shown in Figure 1, is considered. The following state matrix is assumed for the diffusive network process: $A =$

$$\begin{bmatrix} -1 & 1 & 0 & 0 & 0 & 0 & 0 \\ 0 & -1/6 & 1/6 & 0 & 0 & 0 & 0 \\ 1/2 & 1/2 & -1.125 & 0.125 & 0 & 0 & 0 \\ 0 & 0 & 0.25/3 & -2.25/3 & 1/3 & 1/3 & 0 \\ 0 & 0 & 0 & 1/2 & -1.25 & 1/2 & 0.5/2 \\ 0 & 0 & 0 & 1 & 1 & -2 & 0 \\ 0 & 0 & 0 & 0 & 0.5/8 & 0 & -0.5/8 \end{bmatrix}.$$

To evaluate the influence of sensor and actuator position on control performance, three control architecture are considered. First, a fixed architecture where the sensor and actuator are both fixed at at a central node (Node 3) is considered. This fixed scheme is compared with the incidental-measurement architecture and the mobile measurement and actuation architecture studied in this work. For both architectures, the transition probabilities for the location Markov chain are assumed to be $P_{ii} = 0.95$ for $i = 1, \dots, 7$, $P_{ij} = \frac{1}{120}$ for $i \neq j$. For the incidental-measurement architecture, the actuator is assumed to be fixed at node 3. The regulation goal is $y_{ref} = 0$, and the initial condition is $x(0) = [-30, 12, -20, 20, 40, 30, 50]^T$. A time-step $T = 1$ is assumed.
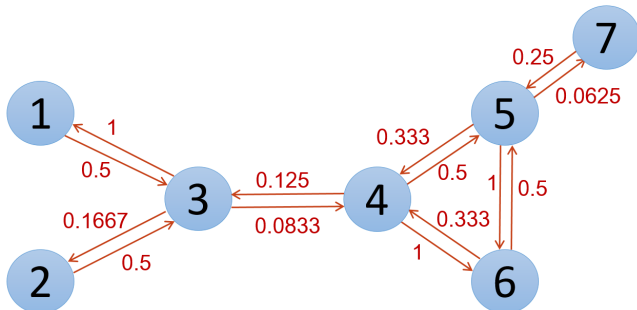

Fig. 1: Topology of the diffusive network model.

Figure 2 show simulations of the state dynamics in the given example, for the three case studies. Control gains are chosen as $K_p = 0.72$, $K_i = 0.01$ and $K_d = 0.02$. The simulations demonstrate that the controller is able to drive all nodes'states to the reference signal, for all three controller architectures. Figure 2a shows that the fixed architecture requires significant time for regulation. In particular, since there is a weak connection between nodes 3 and 4, the states of nodes 4, 5, 6 and 7 have delay in reaching the desired value. The incidental measurement architecture achieves faster regulation, albeit at the cost of increased variability in the interim Fig (3.b). Faster regulation is possible because the measurement device visits nodes that are far from actuation location, which forces the control system to modulate the actuation in response to deviations at these remote locations.

Finally, the mobile measurement-actuation architecture allows much faster regulation, without overshoot. The example indicates that controls using incidental measurements and actuation may be practical for control of complex network processes. Development of formal performance bounds for the incidental measurement/actuation architectures is an important direction of further work.
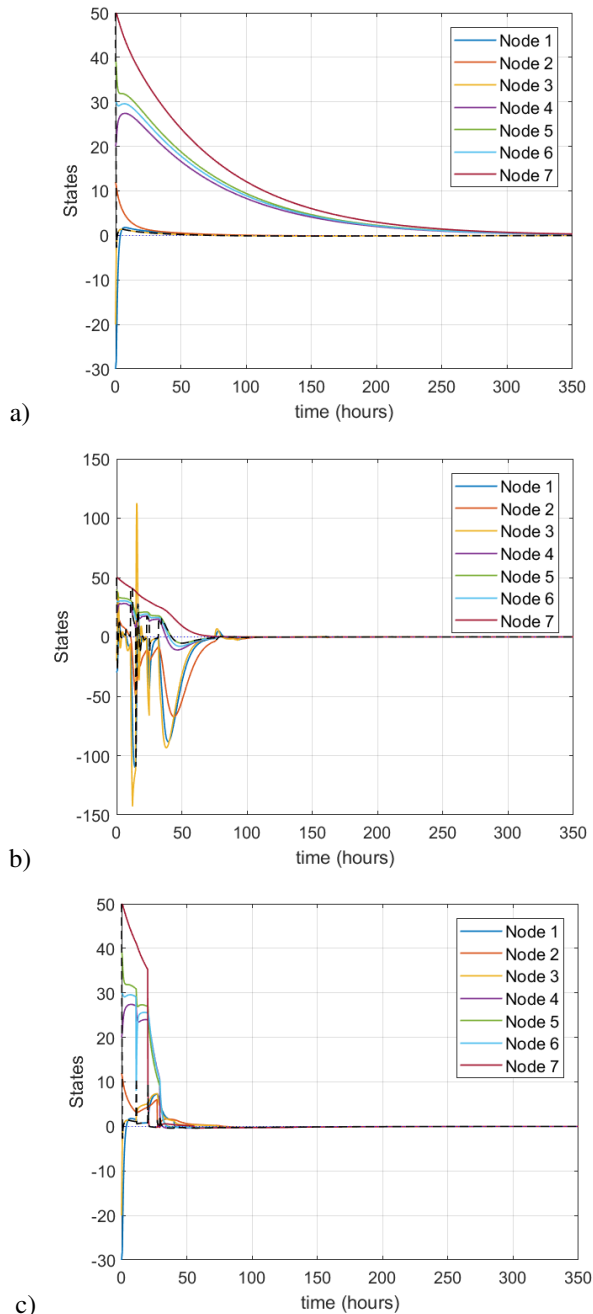

a)

b)

c)

Fig. 2: The state dynamics of the example diffusive network model are shown, the three control architectures: a) fixed actuator and sensor in room 3 ; b) incidental measurements with fixed actuator in room 3 ; c) mobile measurement and actuation. In all figures, location of the measurement device at each time instance is indicated using a dashed line.

V. Conclusions

Regulation of diffusive network processes using incidental measurement- and actuation- based feedback control architectures has been studied. First- and second- moment stability upon application of low-gain PID controllers has been proved. The numerical simulation illustrates differences between the two introduced incidental measurement and actuation paradigms, and suggests that these paradigms may perform well compared to traditional fixed control schemes.

References

[1] Wu, Chai Wah, & Leon O. Chua. "Synchronization in an array of linearly coupled dynamical systems." *IEEE Transactions on Circuits and Systems I: Fundamental Theory and Applications* 42, no. 8 (1995): 430-447.

[2] Wang, Xiao Fan, & Guanrong Chen. "Pinning control of scale-free dynamical networks." Physica A: Statistical Mechanics and its Applications 310, no. 3 (2002): 521-531.

[3] Deng, Kun, Prabir Barooah, Prashant G. Mehta, & Sean P. Meyn. "Building thermal model reduction via aggregation of states." In *Proceedings of the American Control Conference (ACC)* pp. 5118-5123. IEEE, 2010.

[4] Abad Torres, Jackeline, Sandip Roy, & Yan Wan. "Sparse Resource Allocation for Linear Network Spread Dynamics." *IEEE Transactions on Automatic Control* 62, no. 4 (2017): 1714-1728.

[5] Schenato, Luca, & Giovanni Gamba. "A distributed consensus protocol for clock synchronization in wireless sensor network." In Decision and Control, 2007 46th IEEE Conference on, pp. 2289-2294. IEEE, 2007.

[6] Peymani, Ehsan, Hvard Fjr Grip, & Ali Saberi. "Homogeneous networks of non-introspective agents under external disturbances-H almost synchronization." Automatica 52 (2015): 363-372.

[7] Xue, Mengran, Wei Wang, & Sandip Roy. "Security concepts for the dynamics of autonomous vehicle networks." *Automatica* 50, no. 3 (2014): 852-857.

[8] Briegel, Benjamin, Daniel Zelazo, Mathias Brger, & Frank Allgwer. "On the zeros of consensus networks." In *2011 IEEE Conference on Decision and Control and European Control Conference (CDC-ECC)*, 2011.

[9] Abad Torres, Jackeline, & Sandip Roy. "Graph-theoretic analysis of network inputoutput processes: Zero structure and its implications on remote feedback control." *Automatica* 61 (2015): 73-79.

[10] Gubbi, J., Buyya, R., Marusic, S., & Palaniswami, M. (2013). Internet of Things (IoT): A vision, architectural elements, and future directions. Future Generation Computer Systems, 29(7), 1645-1660.

[11] Wei, C., & Li, Y. (2011, September). Design of energy consumption monitoring and energy-saving management system of intelligent building based on the internet of things. In Electronics, Communications and Control (ICECC), 2011 International Conference on (pp. 3650-3652). IEEE.

[12] Mainetti, L., Patrono, L., & Vilei, A. (2011, September). Evolution of wireless sensor networks towards the internet of things: A survey. In Software, Telecommunications and Computer Networks (SoftCOM), 2011 19th International Conference on (pp. 1-6). IEEE.

[13] Sadilek, Adam, Henry A. Kautz, & Vincent Silenzio. "Predicting disease transmission from geo-tagged micro-blog data." In AAAI. 2012.

[14] Herrera, Juan C., Daniel B. Work, Ryan Herring, Xuegang Jeff Ban, Quinn Jacobson, & Alexandre M. Bayen. "Evaluation of traffic data obtained via GPS-enabled mobile phones: The Mobile Century field experiment." Transportation Research Part C: Emerging Technologies 18, no. 4 (2010): 568-583.

[15] S. Roy & R. Dhal, Situational Awareness for dynamical network processes using incidental measurements, IEEE Journal of selected topics in signal processing, Vol. 9, No. 2, March 2015.

[16] A. Vosughi, M. Xeu & S. Roy. (2017). Occupant-Location-Catered Control of IoT-Enabled Building HVAC Systems, 5th IEEE Global Conference on Signal and Information Processing, Montreal, Canada.

[17] Feng, X., Loparo, K. A., Ji, Y., & Chizeck, H. J. (1992). Stochastic stability properties of jump linear systems. IEEE Transactions on Automatic Control, 37(1), 38-53.

[18] Costa, O. L. V., Fragoso, M. D., & Marques, R. P. (2006). Discrete-time Markov jump linear systems. Springer Science and Business Media.

[19] de Farias, D. P., Geromel, J. C., do Val, J. B., & Costa, O. L. V. (2000). Output feedback control of Markov jump linear systems in continuous-time. IEEE Transactions on Automatic Control, 45(5), 944-949.

[20] Roy, S. & Saberi, A. (2005). Static decentralized control of a single-integrator network with Markovian sensing topology. Automatica, 41(11), 1867-1877.

[21] Roy, S., Verghese, G. C., & Lesieutre, B. C. (2006). Moment-linear stochastic systems. In Informatics in Control, Automation and Robotics I (pp. 263-271). Springer Netherlands.

[22] Santesso, P., & Valcher, M. E. (2007). On the zero pattern properties and asymptotic behavior of continuous-time positive system trajectories. Linear algebra and its applications, 425(2), 283-302.

[23] Berman, A., & Plemmons, R. J. (1994). Nonnegative matrices in the mathematical sciences. Society for Industrial and Applied Mathematics.